Acoustic transfer admittance of cylindrical cavities in infrasonic frequency range

P. Vincent, D. Rodrigues, F. Larsonnier, Cécile Guianvarc'H, Stéphane Durand

Acoustic transfer admittance of cylindrical cavities in infrasonic frequency range

To cite this article: P Vincent *et al* 2019 *Metrologia* **56** 015003

View the article online for updates and enhancements.

Acoustic transfer admittance of cylindrical cavities in infrasonic frequency range

P Vincent[1,2], D Rodrigues[2], F Larsonnier[1], C Guianvarc'h[3] and S Durand[4]

[1] Commissariat à l'Énergie Atomique (CEA), DAM, DIF, F-91297 Arpajon, France

[2] Laboratoire Commun de Métrologie LNE-CNAM (LCM), 29 Avenue Roger Hennequin, 78197 Trappes Cedex, France

[3] Laboratoire Commun de Métrologie LNE-CNAM (LCM), 61 Rue du Landy, 93210 La Plaine Saint Denis, France

[4] Laboratoire d'Acoustique de l'Université du Mans (LAUM), UMR CNRS 6613, Avenue Olivier Messiaen, 72085 Le Mans Cedex 9, France

E-mail: paul.vincent@cea.fr

CrossMark

Abstract

Demand for calibration at infrasonic frequencies has emerged in response to earth monitoring problems. The primary standard for sound pressure is defined through the reciprocity calibration method specified in the International Electrotechnical Commission (IEC) Standard 61094-2:2009. This method is based on the use of closed couplers and is routinely applied by the National Metrology Institutes for a large frequency range; however, infrasonic frequencies below 2 Hz have not been explored until recently. The acoustic transfer admittance of the coupler, including the heat conduction effects of the fluid, must be modelled precisely to obtain accurate microphone sensitivity. IEC 61094-2:2009 provides two standardised solutions for the correction of heat conduction. However, researchers have noted significant deviations between these corrections at low frequencies in plane wave couplers, indicating that one or both techniques incorrectly calculate the influence of heat conduction. In this paper, the limitations of the standardised formulations at infrasonic frequencies are identified and two alternative solutions are proposed. An experiment is also reported, which highlights the discussed limitations of the standardised formulations for acoustic transfer admittance, while also demonstrating the validity of the proposed alternative formulations at frequencies down to 0.04 Hz.

Keywords: infrasound, calibration, microphones, reciprocity, coupler, admittance

(Some figures may appear in colour only in the online journal)

1. Introduction

The pressure reciprocity calibration method as specified in the International Electrotechnical Commission (IEC) Standard 61094-2:2009 [1] is currently used worldwide for absolute pressure calibration of laboratory standard microphones, and provides the basis for primary measurement standards for sound pressure. This method, which is based on the use of closed couplers, is routinely applied by the National Metrology Institutes at frequencies of up to 25 kHz and, recently, down to 2 Hz [2]. While the reciprocity method has been used for a long time to determine microphone pressure sensitivity over an extended audible frequency range, the demand for calibration at infrasonic frequencies below 2 Hz has not been identified until recently. This is revealed by the absence of calibration and measurement capabilities (CMCs) in the Bureau International des Poids et Mesures (BIPM) database [3] for frequencies below 2 Hz, except for static pressures, for which CMCs have been obtained using specific techniques such as the pressure balance [4] (see figure 1).
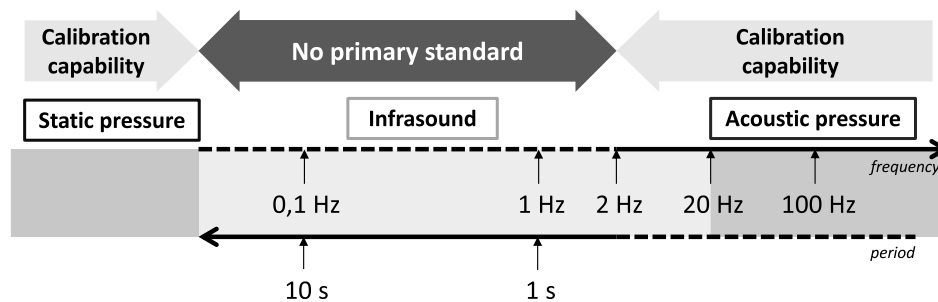
Figure 1. CMC status from static pressure range to acoustic pressure range.

Demand for measurements and calibration at infrasonic frequencies has recently emerged [5, 6] in response to problems such as volcano, tsunami, avalanche, wind turbine, and transportation monitoring [7, 8]. Another key issue pertains to the requirements of the Comprehensive Nuclear Test Ban Treaty Organisation (CTBTO), which provides global international coverage to help enforce nuclear testing bans. The International Monitoring System of the CTBTO requires calibration (amplitude and phase) of its infrasound sensor network in the frequency range of 0.02–4 Hz [9]. Recognising these challenges, the Consultative Committee for Acoustics, Ultrasound and Vibration (CCAUV) of the BIPM noted the need for acoustic calibration capabilities at frequencies below 20 Hz in its latest strategic document for the period of 2017–2027 [10].

To perform calibration at infrasonic frequencies, the validity and performance of the pressure reciprocity method must be examined for this frequency range. In the most usual configuration, the pressure reciprocity method requires three reciprocal microphones coupled by pairs using a cavity, generally with a cylindrical shape. The coupler ends are closed by the microphone diaphragms, with one being used as a transmitter and the other one as a receiver. The product of the microphone sensitivities is determined from electrical measurements and from analytical calculation of the acoustic transfer admittance of the system. This operation is repeated with three microphone couples.

Calculation of the acoustic transfer admittance is a key aspect of microphone pressure reciprocity calibration. The acoustic transfer admittance, defined as the ratio of the short-circuit volume velocity produced by the transmitter microphone to the sound pressure acting on the diaphragm of the receiver microphone has been extensively explored and discussed considering both influence of heat conduction and viscous losses [11–21]. In particular, the effects of heat conduction is an important issue of the calculation of the acoustic transfer admittance especially in small closed volumes and at low frequencies where the expansion and compression processes of the gas are somewhere in between an isothermal process and an adiabatic one, or said to be polytropic process. The IEC Standard 61094-2:2009 [1] provides two formulations for calculation of the acoustic transfer admittance. These formulations have been revised in the context of the above problem since the first edition, IEC 327 [22], which was published in

1971. However, significant behavioural differences between the standardised models at very low frequencies have recently been highlighted; these discrepancies yield to inconsistent calibration results [19, 20].

With the objective of achieving an acoustic primary standard in the infrasonic frequency range, the second section of this paper discusses the limitations of the standardised acoustic transfer admittance formulations and proposes alternatives. The second section highlights these limitations and the validity of the proposed alternative formulations by reporting an experimental study in the frequency range of 0.04–100 Hz. A detailed presentation of the measurement setup and methodology is provided, and the experiment results are reported and discussed.

2. Acoustic transfer admittance: model presentation

The IEC Standard 61094-2:2009 [1] specifies the requirements for pressure reciprocity calibration of laboratory standard (LS) microphones and includes models for calculating the acoustic transfer admittance of cylindrical couplers. In appendix A of the standard, two formulations for correcting heat conduction under polytropic conditions are presented:

(a) the *'broadband solution'*, which considers both thermal and viscous effects in plane wave couplers and is applicable to higher frequencies;

(b) the *'low-frequency solution'*, which considers only thermal effects for cylindrical coupler assuming uniform pressure, and which is based on a solution presented by Gerber [13].

Recently, Jackett [20] highlighted significant deviations between these models at low frequencies for plane wave couplers, indicating that one or both models incorrectly calculate the influence of heat conduction.

To realise a primary standard for the infrasonic frequency range, validation of an appropriate acoustic modelling technique appears to be an essential preliminary step. The two standardised models are based on the fundamental equations of acoustics in thermo-viscous fluids, with simplification of these equations through adoption of several hypotheses to avoid overly intricate problem formulation. These hypotheses are discussed below.
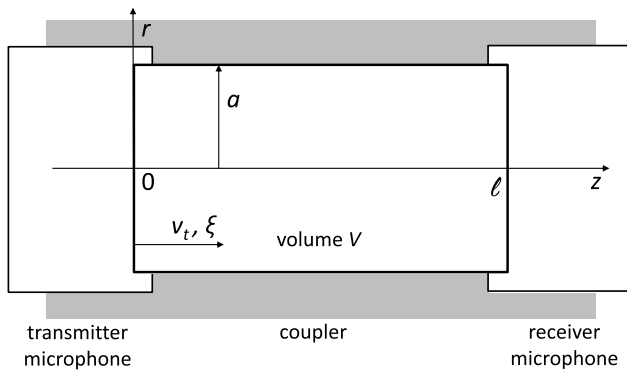
Figure 2. Coupler geometry with the two microphones.

2.1. IEC 61094-2:2009: the 'broadband solution'

At high frequencies, use of the IEC standardised 'broadband solution' is usually recommended; this solution is appropriate for a cylindrical coupler with the same diameter as the microphone membrane.

The considered system is a cylindrical cavity (length ℓ, radius a) closed at one end $z = 0$ by the diaphragm of a transmitter microphone driven by a displacement field ξ and velocity $v_t = j\omega\xi$ (where ω is the angular frequency) and at the other end $z = \ell$ by the diaphragm of a receiver microphone (figure 2). For calibration of 1 inch microphones, the lengths of cavities typically range 12–34 mm.

According to [1], at frequencies for which plane wave transmission can be assumed in the coupler, the propagation in the coupler can be considered as a homogeneous transmission line. The acoustic transfer admittance Y_a can then be written as

$$Y_a = \left(Y_r + Y_t \right) \cosh(k\,\ell) + \left(\frac{1}{Z_0} + Y_r Y_t \right) \sinh(k\,\ell), \tag{1}$$

where Z_0 is the iterative impedance; k the complex wave number; Y_r and Y_t the acoustical admittances of receiver and transmitter microphones, respectively; and ℓ the coupler length.

For a cylinder, the complex wave number and the iterative impedance, which take into account both thermal and viscous effects, can be expressed as

$$k = \frac{j\omega}{c_0} \left(1 + \frac{1-j}{a\sqrt{2}} \left(\sqrt{\frac{\eta}{\omega\rho}} + (\gamma - 1)\sqrt{\frac{\alpha_t}{\omega}} \right) \right),$$
$$Z_0 = \frac{\rho_0 c_0}{S_0} \left(1 + \frac{1+j}{a\sqrt{2}} \left(\sqrt{\frac{\eta}{\omega\rho}} - (\gamma - 1)\sqrt{\frac{\alpha_t}{\omega}} \right) \right), \tag{2}$$

where S_0 is the cylinder section, ρ_0 the gas static density, c_0 the speed of sound, γ the ratio of the specific heat capacities, α_t the thermal diffusivity of the enclosed gas, and η the air viscosity.

The equations provided above take into account only losses at the cylindrical surface. To incorporate heat conduction losses that occur at the boundary surfaces, the IEC standard suggests adding an admittance Y_b can be added to each microphone admittance Y_r and Y_t, where

$$Y_b = \frac{S_0}{\rho_0 c_0} \frac{1+j}{\sqrt{2}} (\gamma - 1) \frac{1}{c_0} \sqrt{\alpha_t \omega}. \tag{3}$$

Hence, the following expression for the acoustic transfer admittance is obtained:

$$Y_a = \left(2Y_b + Y_r + Y_t \right) \cosh(k\,\ell) + \left(\frac{1}{Z_0} + (Y_r + Y_b)(Y_t + Y_b) \right) \sinh(k\,\ell). \tag{4}$$

The 'broadband solution' has been developed based on a revisited and coherent description constructed from analytical results available in the literature (essentially, Kirchhoff's theory) [15, 23]. Previously, Guianvarc'h *et al* [18] reported accurate development of this model, which is of interest here to elucidate the limitations of modelling in the infrasound context. The standardised model is constructed from the fundamental equations of acoustics in thermo-viscous fluids: (a) the Navier–Stokes equation [18, equation (1)], (b) the conservation of mass equation [18, equation (2)], and (c) the Fourier for heat conduction [18, equation (3)]. As mentioned above, these equations are simplified by adopting several hypotheses for simpler problem formulation. In particular, the system of equations is simplified by considering a quasi plane wave approximation. Essentially, in the cylindrical coordinate system, the spatial derivatives of the temperature variation and of the particle velocity with respect to the azimuth and height coordinates in the Fourier equation and in the Navier–Stokes equation, respectively, are much smaller than the derivative with respect to the radial coordinate:

$$\left| \frac{\partial \tau}{\partial r} \right| \gg \left| \frac{\partial \tau}{\partial z} \right| \text{ and } \left| \frac{\partial \tau}{\partial r} \right| \gg \left| \frac{\partial \tau}{\partial \theta} \right|, \tag{5}$$

$$\left| \frac{\partial v}{\partial r} \right| \gg \left| \frac{\partial v}{\partial z} \right| \text{ and } \left| \frac{\partial v}{\partial r} \right| \gg \left| \frac{\partial v}{\partial \theta} \right|, \tag{6}$$

with τ the temperature variation, v the particle velocity, and (r, θ, z) the cylindrical coordinate system. These assumptions lead to the simplified equations (10) and (11) in [18]. In particular, the assumption on the temperature variation presented here in (5) conducts to write the solution for the Fourier equation as the solution for an 'infinite tube' [18, equation (13)].

However, as the thermal boundary layer thickness δ_h is inversely related to the square root of the frequency:

$$\delta_h \approx \sqrt{\frac{2\alpha_t}{\omega}}, \tag{7}$$

the considered assumption (5) and thus the simplification of the Fourier equation [18, equation (11)] are no longer valid in the infrasonic frequency range, as the thermal boundary layer increases when the frequency decreases. In general, this simplified assumption can be considered to be valid when δ_h is much smaller than the typical coupler dimensions:

$$\delta_h \ll \sqrt[3]{V}, \tag{8}$$

where V is the coupler volume. As an example, δ_h reaches 8.2 mm at 0.1 Hz, which is significant compared to the typical

dimensions of couplers used for reciprocity calibrations [1, appendix C].

This simplified formulation seems applicable to the description of the particle velocity over a large frequency range including lower frequencies, given the typical dimensions of couplers used for reciprocity calibration (when $\omega\rho a^2 > 100\eta$ [1]).

In addition, the cylindrical-cavity the acoustic impedance of the plane waves in the coupler Z_0 and the complex wave number k provided in the IEC standard correspond to asymptotic developments of general formulations [18, equations (23) and (24d)]. These formulations are valid only under assumption of a 'large tube', when the thermal boundary layers are neglected compared to the radius of the cylindrical coupler.

Consequently, the discussion developed above suggests that the 'broadband solution' quoted in IEC Standard 61094-2:2009 is inappropriate for microphone reciprocity calibration in the infrasonic frequency range.

2.2. IEC 61094-2:2009: the 'low-frequency solution'

At low frequencies, IEC Standard 61094-2:2009 recommends use of the 'low-frequency solution', which is assumed to be appropriate for any cylindrical coupler if the pressure in the cavity is assumed to be uniform. In this case, the acoustic transfer admittance Y_a is given by

$$Y_a = j\omega\frac{V}{\gamma P_0}\Delta_H + Y_r + Y_t,\tag{9}$$

where P_0 is the static pressure under measurement conditions. The thermal correction Δ_H applied to the volume V is expressed as

$$\Delta_H = \frac{\gamma}{1 + (\gamma - 1)E_V},\tag{10}$$

where

$$E_V = 1 - X_V + \frac{\pi R^2 + 8R}{\pi(2R+1)^2}X_V^2 \\ + \frac{3}{4}\sqrt{\pi}\frac{R^3 - 6R^2}{3\sqrt{\pi}(2R+1)^3}X_V^3,\tag{11}$$

with

$$X_V = \frac{A}{V}\frac{1-j}{\sqrt{2}}\sqrt{\frac{\gamma\alpha_t}{\omega}},\tag{12}$$

where $R = \ell/(2a)$ and A is the total internal area of the cylinder surface.

This specific formulation is based on one of the two solutions provided by Gerber [13], who solved the thermo-acoustic problem by considering the Fourier equation for heat conduction with no thermal source inside the domain:

$$\left(\frac{\partial}{\partial t} - \alpha_t\nabla^2\right)\tau = \frac{\gamma - 1}{\beta\gamma}\frac{\partial p}{\partial t}.\tag{13}$$

For Gerber, p represented the pressure variation produced by an adapted generator. This p was described as the cause of the temperature variation τ in the fluid, with t being time, ∇^2

the Laplacian operator, and β the increase in pressure per unit increase in temperature at constant density.

Furthermore, using the linearised thermodynamic law expressing the density variation as a function of the independent variables p and τ:

$$\rho = \rho_0\chi_T(p - \beta\tau),\tag{14}$$

where $\chi_T = \gamma/(\rho_0 c^2)$ is the bulk isothermal coefficient, from the Fourier equation (13), Gerber also expressed the heat conduction equation as

$$\left(\frac{\partial}{\partial t} - \gamma\alpha_t\nabla^2\right)\tau = \frac{\gamma - 1}{\beta\chi_T\rho_0}\frac{\partial\rho}{\partial t},\tag{15}$$

where, for Gerber, ρ represented the density variation produced by an adapted generator. This ρ was the cause of the temperature variation τ in the fluid.

Gerber proposed solution of the heat conduction equation for the temperature variation τ by considering two different interpretations:

(1) The pressure variation p produced by a pressure generator (zero impedance driver) is the cause of the temperature variation τ; this p was assumed to be uniform in the coupler and to characterise the source of the acoustic field in (13);

(2) The density variation ρ produced by a flow generator (infinite impedance driver) is the cause of the temperature variation τ; this ρ was assumed to be uniform in the coupler and to characterise the source of the acoustic field in (15).

It is the second interpretation featuring the infinite impedance driver that yields (10) for the thermal correction Δ_H, which is included in the current edition of IEC Standard 61094-2:2009 for the 'low-frequency solution' and was featured in the previous, 1992 edition [24].

The presentation of two different mathematical problems for the unique acoustic problem of the cavity raises questions about the relevance of the formulation defined by Gerber. In [18, 25], Guianvarc'h proposed an analysis of these interpretations that is performed in this paper.

(a) Gerber interpreted the Fourier equation for heat conduction as a diffusion equation in which the second term involving the pressure variation p (13) or the density variation ρ (15) expresses the contribution of a given source (a zero impedance driver or infinite impedance driver) to the diffusion process. This approach does not appear to be appropriate as the pressure variation p or the density variation ρ in the heat conduction equation does not represent the influence of a source, but rather describes the thermodynamic state of the fluid in the cavity. To adopt a rigorous approach, if a thermal source is acting within the domain, its contribution should be incorporated via an additional term h [26, section 2.5.1] in the second member of the heat conduction equation (13). Furthermore, if a source is acting on the boundaries of the domain, it should be considered in the boundary conditions. In other words, the Fourier equation (13) and the modified Fourier equa-

tion (15) only make the links between the temperature variation and respectively the pressure variation and the density variation in the domain. These equations do not contain any information or specification about the sound source. Consequently, the interpretation assuming that the pressure variation p or the density variation ρ in the heat conduction equation represents the influence of a zero or infinite impedance driver, respectively, is inappropriate. This problem could generate confusion in selecting between the two interpretations provided by Gerber. Indeed, a review of the available literature suggests that the inclusion of the second Gerber interpretation (with an infinite impedance driver) in the 1992 and 2009 editions of the IEC Standard 61094-2 was based on [16]. In that work, the author recommended the second interpretation because the acoustic impedance of a microphone calibrated based on the reciprocity method is usually very high.

(b) In the second interpretation (for an infinite impedance driver), it is assumed that the time-varying density of the fluid does not depend on the coordinates inside the cavity (15). However, this hypothesis is inconsistent with the assumption that the temperature field is non-uniform inside the cavity when the pressure field is uniform in the lower-frequency range, according to the basic thermodynamic laws for gases (14).

(c) The solution (11) given in the current IEC Standard 61094-2 is a short-term Laplace asymptotic development of E_V deduced from a general solution provided by Gerber [13, 24b]. Such a development can only be valid if the angular frequency ω is not too small, as X_V is proportional to $1/\omega$. This short-term solution becomes inappropriate when the frequency decreases further in the infrasonic frequency range. As an example, in the case of a 6 mm high and 18.6 mm diameter cavity with two Brüel & Kjæ r (B&K) Type 4160 microphones, the error on $\|E_V\|$ obtained for the short-term development (11) compared to the complete solution [13] is more than 0.1 dB when the frequency is lower than 0.4 Hz.

The above discussion suggests that the 'low-frequency solution' quoted in IEC Standard 61094-2:2009 is inappropriate for microphone reciprocity calibration, particularly in the infrasonic frequency range. In the next subsection, an alternative formulation is presented with the aim of overcoming these limitations.

2.3. Alternative low-frequency solution

The variables describing the dynamic and thermodynamic states of the fluid are the particle velocity v, the entropy variation σ, the pressure variation p, the density variation ρ, and the temperature variation τ. The parameters that specify the properties and nature of the fluid are the ambient values of the density ρ_0, the static pressure P_0, the shear viscosity coefficient μ, the bulk viscosity coefficient η, and the coefficient of thermal conductivity λ.

The complete set of linearised homogeneous equations governing small-amplitude disturbances of the fluid includes the following equations.

– **Navier–Stokes equation**
Without the force source, this equation can be expressed as

$$\frac{1}{c_0}\frac{\partial v}{\partial t} + \frac{1}{\rho_0 c_0}\nabla p = \ell_v \nabla\left(\nabla \cdot v\right) - \ell'_v \nabla \times \left(\nabla \times v\right), \quad (16)$$

where ℓ_v and ℓ'_v are characteristic lengths defined by

$$\ell_v = \frac{1}{\rho_0 c_0}\left(\frac{4}{3}\mu + \eta\right) \quad \text{and} \quad \ell'_v = \frac{\mu}{\rho_0 c_0},$$

and $c_0 = \sqrt{\gamma/\rho_0 \chi_T}$ is the speed of sound. When the cavity dimensions are considered to be much lower than the acoustic wavelength, the pressure field can be assumed to be uniform everywhere inside the cavity, even within the viscous and thermal boundary layers. Thus, $\nabla p = 0$, the particle velocity v is close to zero at any point of the cavity, and the viscosity effect vanishes. In fact, the Navier–Stokes equation is not required in this formulation.

– **Conservation of mass equation**
The conservation of mass equation can be integrated over the entire cavity volume [18]:

$$\iiint_V \frac{\partial \rho}{\partial t}\,\mathrm{d}V + \rho_0 \iint_A v\,\mathrm{d}A = 0. \quad (17)$$

As some cavity walls are driven by a vibratory displacement motion (herein, $z = 0$, for the transmitter microphone diaphragm) and others are characterised by their impedance Z (pressure/velocity; herein, $z = \ell$, for the receiver microphone), this equation takes the following form:

$$\iiint_V \rho\,\mathrm{d}V + \rho_0 \iint_A \xi\,\mathrm{d}A + \frac{\rho_0}{j\omega}\iint_A \frac{p}{Z}\,\mathrm{d}A = 0. \quad (18)$$

As the pressure field is assumed to be uniform, it can be expressed as follows:

$$\frac{1}{\rho_0}\iiint_V \rho\,\mathrm{d}V + \delta V + \frac{pA}{j\omega Z} = 0, \quad (19)$$

where the mean admittance $1/Z$ is defined as

$$\iint_A \frac{p}{Z}\,\mathrm{d}A = p\iint_A \frac{1}{Z}\,\mathrm{d}A = \frac{pA}{Z}. \quad (20)$$

The cavity volume variation δV is due to the displacement field of the transmitting diaphragm; therefore,

$$\delta V = \iint_S \frac{v}{j\omega}\,\mathrm{d}S = -S_0 \xi. \quad (21)$$

– **Basic thermodynamic laws for gases**
The combination of the linearised thermodynamic law expressing the density variation (14) with (20) yields

$$\left(1 + \frac{A}{j\omega Z \chi_T V}\right) p - \frac{\beta}{V} \int\int\int_V \tau \, \mathrm{d}V = \frac{\delta V}{\chi_T}. \quad (22)$$

In particular, this equation shows that the pressure field does not depend on $\tau(r, z, t)$, but rather on its average value over V, while the temperature variation τ changes significantly within the boundary layers.

– **Fourier equation for heat conduction**

The Fourier equation for heat conduction is given by (13), considering the thermodynamic law expressing the entropy variation as a function of the independent variables p and τ. Insofar as the acoustic pressure field is assumed to be uniform in the cavity, the solution of this equation with $\tau = 0$ on the boundaries and for an axisymmetric problem (i.e. where the solution does not depend on the azimuthal coordinate) was provided by Gerber [13], for the average value of τ over V:

$$\langle\tau\rangle = p \, \frac{\gamma - 1}{\beta\gamma} E_P, \quad (23)$$

where E_P is given by the general solution formulation

$$E_P = \sum_{m=0}^{+\infty} \sum_{n=1}^{+\infty} \left[\frac{8/\pi^2}{(m + 1/2)^2 \lambda_n^2} F_{m,n}\right],$$

$$\text{with } F_{m,n} = \left(1 + \frac{\lambda_n^2 R^2 + (m + 1/2)^2 \pi^2}{(1 + 2R)^2} X_P^2\right)^{-1}. \quad (24)$$

A short-term Laplace asymptotic development of the previous general solution can also be obtained:

$$E_P = 1 - X_P + \frac{\pi R^2 + 8R}{\pi(2R + 1)^2} X_P^2$$
$$+ \frac{3}{4}\sqrt{\pi} \frac{R^3 - 6R^2}{3\sqrt{\pi}(2R + 1)^3} X_P^3, \quad (25)$$

where

$$X_P = \frac{A}{V} \frac{1 - j}{\sqrt{2}} \sqrt{\frac{\alpha_t}{\omega}}. \quad (26)$$

It is worth noting that the pressure variation p in the second term of the heat conduction equation here describes the thermodynamic state of the fluid in the cavity and does not represent the influence of a source.

Combining (23) with (22), the pressure variation in the cavity is given by

$$p = -\frac{\delta V}{\chi_T V} \frac{1}{1 + \frac{1}{j\omega \chi_T V} Y_r - \frac{\gamma - 1}{\gamma} E_P}, \quad (27)$$

where the ratio A/Z is developed as

$$\frac{A}{Z} = \int\int_A \frac{1}{Z} \mathrm{d}A = \int\int_S \frac{Y_r}{\pi a^2} \mathrm{d}S$$
$$= \int_0^{2\pi} \int_0^a \frac{Y_r}{\pi a^2} r \, \mathrm{d}r \, \mathrm{d}\theta = Y_r. \quad (28)$$

Note that acoustic transfer admittance Y_a is defined as the 'quotient of the short-circuit volume velocity produced by the

microphone used as a transmitter by the sound pressure acting on the diaphragm of the microphone used as a receiver' [1]. That is,

$$Y_a = \frac{Sv_t + Y_t p(0)}{p(\ell)} = \frac{-j\omega \delta V}{p} + Y_t. \quad (29)$$

Invoking (27) for the acoustic pressure and assuming the fluid is a perfect gas ($\gamma/\chi_T \approx \gamma P_0$), we straightforwardly obtain

$$Y_a = \frac{j\omega V}{\gamma P_0} \left[\gamma - (\gamma - 1)E_P\right] + Y_r + Y_t. \quad (30)$$

This solution is equivalent to that provided by the first Gerber interpretation [13] (for a zero impedance driver). However, (30) incorporates the admittance of the receiver microphone by considering the formulation of the conservation of mass equation. Therefore, we make no claims of novelty here. However, the present effort towards formulation clarity should be of some interest.

Similar to the previous discussion regarding the short-term Laplace asymptotic development of E_V (11), the short-term Laplace asymptotic development of E_P (25) should be inappropriate as the frequency decreases, especially to the infrasonic frequency range. Thus, the general formulation of E_P (24) should be preferred for the lowest frequencies.

2.4. Model comparison

The four models of the acoustic transfer admittance of cylindrical cavities presented above can briefly be summarised as follows:

1. the standardised IEC 61094-2:2009 'broadband solution' (4);
2. the standardised IEC 61094-2:2009 'low-frequency solution' (9) based on the short-term Gerber solution for E_V (11);
3. the *short-term alternative low-frequency solution* (30) based on the short-term Gerber solution for E_P (25);
4. the *general alternative low-frequency solution* (30) based on the Gerber general solution for E_P (24).

Figure 3 presents the theoretical acoustic transfer admittance amplitudes for a 18.6 mm diameter and 6 mm height coupler with two B&K Type 4160 microphones, as given by the four models. The inset is a magnification of the trends for the four models between 1 Hz and 20 Hz.

It is worth noting that, at 1 Hz, the standardised IEC 61094-2:2009 'low-frequency solution' differs significantly from the other models, i.e. by 0.1 dB. At 0.04 Hz, which is the lower frequency limit targeted in this study, the deviations reach several decibels. These deviations between the formulations show that the accuracy of the acoustic modelling of the acoustic transfer admittance is one of the main problems requiring resolution in order to achieve an acoustic primary standard in the infrasonic frequency range. The next section presents an experimental setup designed to estimate the potential validity of the alternative low-frequency solutions discussed hereafter, which also highlights the limits of the standardised formulations.
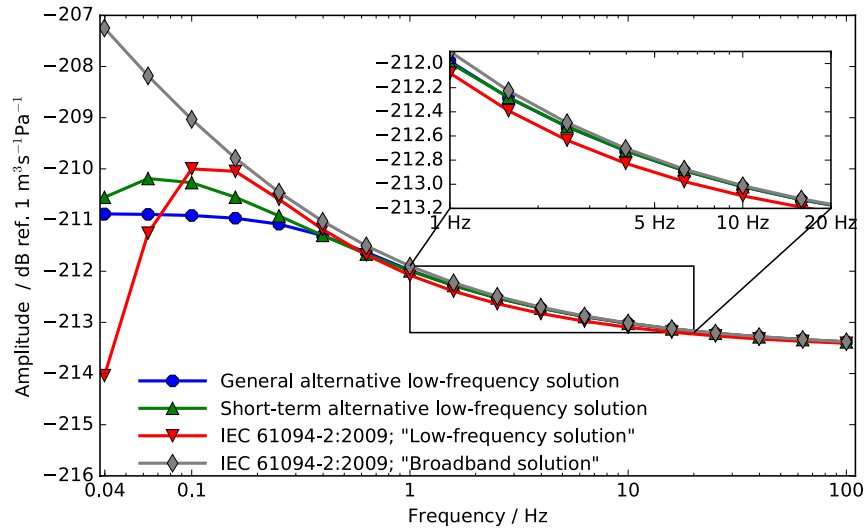
Figure 3. Amplitude (unit: dB ref. 1 m^3 s^{-1} Pa^{-1}) of theoretical acoustic transfer admittance as function of frequency for 6 mm high coupler and two B&K Type 4160 microphones, as given by four models.
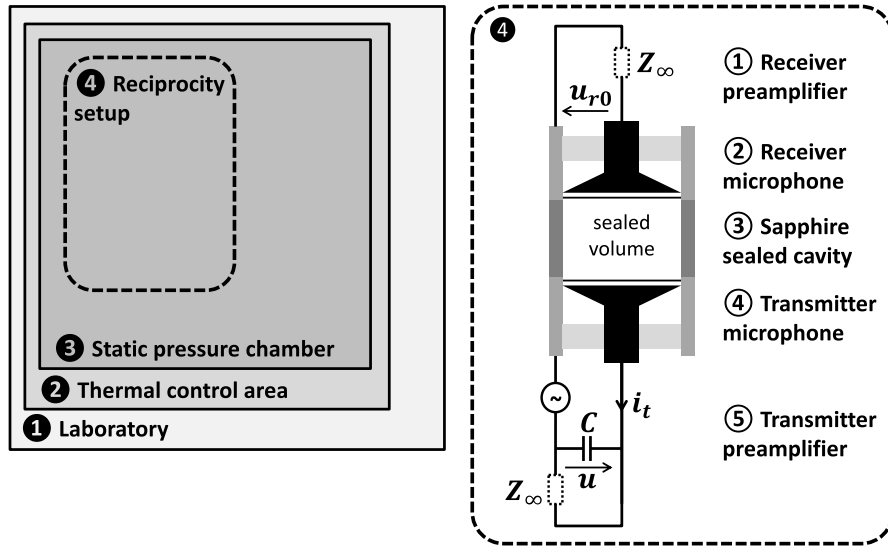
Figure 4. Schematic of measurement setup.

3. Validity test for acoustic transfer admittance formulations

3.1. Methodology

The experimental protocol implemented to test the accuracy of the above formulations for the acoustic transfer admittance was derived from [27] and was based on the pressure reciprocity method. Figure 4 presents an overview of the measurement system. Two electrical transfer impedances (defined as the ratio of the open-circuit voltage u_{r0} of the receiving microphone to the current i_t through the transmitter microphone) were measured for a pair of microphones using two cavities of different lengths, hereafter referred to as the short and long cavities.

The products of the sensitivities M_r and M_t of the receiver and transmitter microphones, respectively, are given by the well-known equations

$$M_t M_r\big|_s = Z_{e,s}\, Y_{a,s}\,,$$
$$\text{and}$$
$$M_t M_r\big|_\ell = Z_{e,\ell}\, Y_{a,\ell}\,, \tag{31}$$

for the short and long cavities (subscripts s and ℓ), respectively. Here, $Y_{a,(s,\ell)}$ are the previously defined and discussed acoustic transfer admittances of the cavities. By considering the microphones as stable during the experiment, the products of the sensitivities $M_t M_r\big|_s$ and $M_t M_r\big|_\ell$ should be invariant as functions of the cavity, insofar as the models of the acoustic transfer admittances are perfectly valid. The objective of the experiment was to test this validity. Therefore, the error estimator δ_m was defined as the ratio

$$\delta_m = \frac{M_t M_r\big|_s}{M_t M_r\big|_\ell} = \frac{Z_{e,s}\, Y_{a,s}}{Z_{e,\ell}\, Y_{a,\ell}}\,. \tag{32}$$
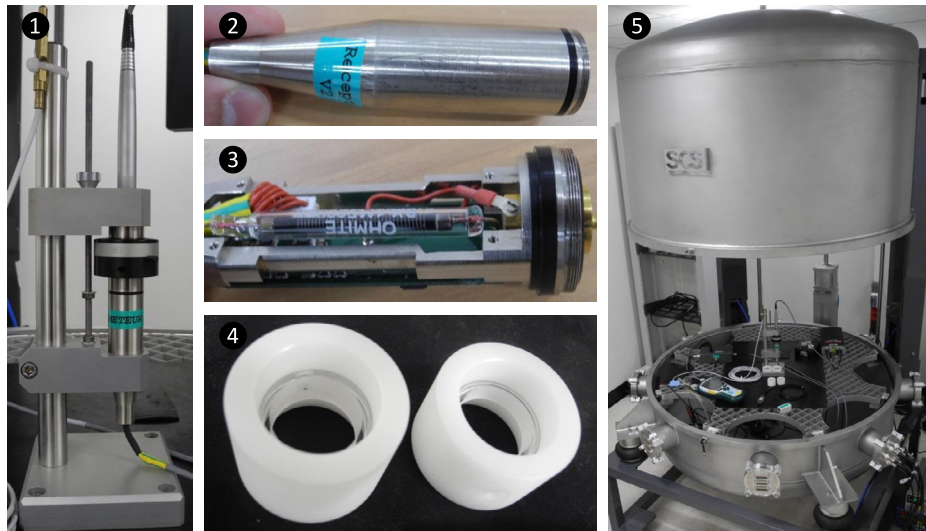
Figure 5. Measurement setup: ❶ reciprocity calibration system with usual cavities, ❷, ❸ IMP preamplifier, ❹ sealed sapphire cavities, and ❺ static pressure chamber.

This ratio should tend towards unity (or 0 dB) for a perfect model of the acoustic transfer admittances $Y_{a,(s,\ell)}$. Otherwise, the estimated $M_t M_r$ depends on the cavity dimensions, so the model is invalid.

During a reciprocity calibration, the electrical transfer impedance is measured using the insert voltage technique [1] to determine the u_{r0} of the receiver microphone. The current i_t through the transmitter microphone is deduced from the voltage developed across a series-connected capacitor $u = i_t/(j\omega C)$, knowing the value of C (figure 4). Thus, the electrical transfer impedance is measured based on two voltage ratios, as follows:

$$Z_e = \frac{-1}{j\omega C} \frac{u_r}{u_t} \frac{u_t'}{u_r'}, \tag{33}$$

where u_r/u_t and u_t'/u_r' are the ratios of voltages measured at the outputs of the microphone power supply of the receiver (u_r and u_r') and transmitter (u_t and u_t') microphones, respectively, during the main measurement phase and voltage insertion phase.

A defined measurement process with two cavities is implemented by fixing the following variables:

– the microphone, preamplifier, and conditioner combinations for the receiver and transmitter;
– the respective settings of the conditioners, assuming that both measurement channels are stable.

Here, the error estimator δ_m is given by

$$\delta_m = \frac{u_{r,s}/u_{t,s}}{u_{r,\ell}/u_{t,\ell}} \frac{Y_{a,s}}{Y_{a,\ell}}, \tag{34}$$

where the subscripts s and ℓ represent the short and long cavities, respectively, in the voltage ratios (hereinafter referred to as the electrical transfer function). Note that this simplification of the measurement process is of interest in the context of infrasound measurement, as these measurements are time-consuming (see related discussion below in section 3.3).

3.2. Measurement setup

As it was essential to perform the experiment in the infrasonic frequency range, i.e. from 0.04 Hz to 100 Hz, some changes were required to the measurement setup employed in this study. The measurements were performed inside a regulated static pressure chamber (figure 5) installed in a laboratory with a dedicated thermally controlled area. This controlled environment was required to avoid microphone instability due to static pressure and temperature changes. Note that this is particularly important for measurements at infrasonic frequencies for which very long integration times are required. Appendix A provides further detail on the environment control setup.

The reciprocity system was composed of two microphones and their preamplifiers, which were sequentially coupled by two sapphire cavities. The transmitter and receiver microphones were two B&K Type 4160 1 inch microphones, which are usually used for pressure reciprocity calibration (LS1p microphones). Two cavities were especially designed and manufactured for the purposes of this study: a short (6 mm long) and long (10 mm long) cavity. Their diameters fit the microphone membranes (18.6 mm) (see figure 5).

The cavity lengths were chosen to be sufficiently different to allow measurement of the deviation between the thermal corrections $\gamma - (\gamma - 1)E_p$ incorporated in (30) for both cavities. For these cavity lengths, the deviation of the thermal corrections reached 0.3 dB in the isothermal-adiabatic transition frequency range; this could be measured with the given reciprocity system accuracy.

The receiver microphone was connected to a B&K 2669-L-004 preamplifier with a parallel 100 pF B&K UC0211 capacitance module. The transmitter microphone was connected to a specific preamplifier designed and manufactured for the purposes of this study (figure 5). The latter had a cut-off frequency of approximately 0.005 Hz given by a 500 GΩ polarisation resistor, with addition of a 100 pF capacitance in parallel with the microphone. Appendix B provides further
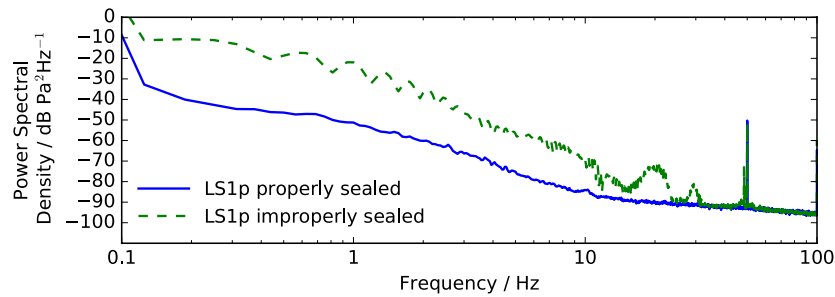
Figure 6. Power spectral density (unit: dB Pa^2 Hz^{-1}) as function of sound pressure frequency measured by receiver microphone for properly and improperly sealed systems.
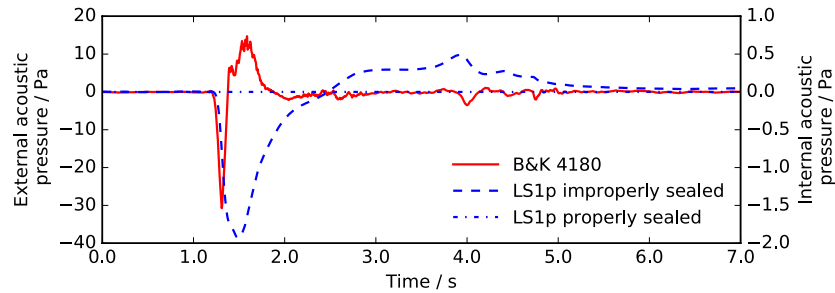
Figure 7. Sample Dirac pressure drop (unit: Pa) in laboratory as function of time. The acoustic pressure inside the laboratory measured with a B&K 4180 microphone (solid line, left *y*-axis), inside a properly sealed reciprocity system (dotted line, right *y*-axis), and inside an improperly sealed reciprocity system (dashed line, right *y*-axis).

detail on the preamplifiers. The output preamplifiers were connected to a 4 channel B&K Type 2829 microphone power supply. This conditioner was modified by bypassing the high-pass filter. The signals were digitised by a VTI Instruments CMX09 chassis and an EMX4350 digitiser card. The digitising system had a negligible noise level compared to that of the signal to be measured. The amplitude and phase of the signals were computed using a standardised method given in [28], as described in appendix C.

To avoid acoustic short-circuiting and to obtain a sufficiently high signal-to-noise ratio at lower frequencies, special attention was paid to the sealing of the reciprocity system. That is, the back cavity vents of both microphones were sealed and the cavities were designed with gaskets to ensure optimal sealing conditions. Appendix B provides further detail on this specific design.

Another reason for sealing the microphones is to simplify the modelling of the microphone acoustic admittances, which is required for all acoustic transfer admittance formulations. Consequently, complex modelling [19] of the microphone vent effects at low frequencies is not required, which places the experiment focus on validation of the thermal effects on the acoustic transfer admittance only. Given the frequency range of interest (lower than 100 Hz), the microphone admittance (Y_t for the transmitter or Y_r for the receiver) of (1), (9), and (30) is given in its simplest form [1] by

$$Y_{r,t} = \frac{j\omega V_{\mathrm{eq},(r,t)}}{\gamma_{\mathrm{ref}}P_{\mathrm{ref}}}, \qquad (35)$$

where $V_{\mathrm{eq},(r,t)}$ is the equivalent volume of the microphones, and γ_{ref} and P_{ref} are the specific heat ratio and static pressure at reference environmental conditions, respectively. For

a fully rigorous discussion, is should be noted that the back cavity of the microphone is also subject to thermal effects and its equivalent volume should be dependent on the frequency when the acoustic behaviour is no longer adiabatic. However, in the experiment conducted in this study, the equivalent volumes of the LS1p microphones were much lower than the volume of the smallest cavity ($V/V_{\mathrm{eq},(r,t)} \approx 20$). Therefore, these complex effects were assumed to be negligible.

One method of obtaining information on the pressure tightness is to measure the self-noise of the receiver microphone. The continuous curve in figure 6 corresponds to the self-noise measurement power spectral density for a properly sealed reciprocity system (30 min integration, recorded after thermal balancing with the receiver microphone). The dashed curve indicates the same measurement without the gaskets in the reciprocity system.

An almost 30 dB deviation can be observed between the properly and improperly sealed reciprocity systems in the infrasonic frequency range. As the self-noise measurement is time-consuming, a quicker method was implemented in this study to avoid measurement for an improperly sealed system. That is, the effects of an energetic pull of the laboratory door were observed in real time. Unlike the case of poor sealing, the reciprocity system tightness was verified if no significant signal was measured by the receiver microphone.

Figure 7 shows sample results for this leak test. The pressure drop in the laboratory was measured by a B&K 4180 microphone (external acoustic pressure: solid line). The dotted and dashed curves correspond to signals from the receiver microphone of the reciprocity system (internal acoustic pressure) when the gaskets were properly (dotted line) and improperly (dashed line) placed. The amplitude of the signal inside the
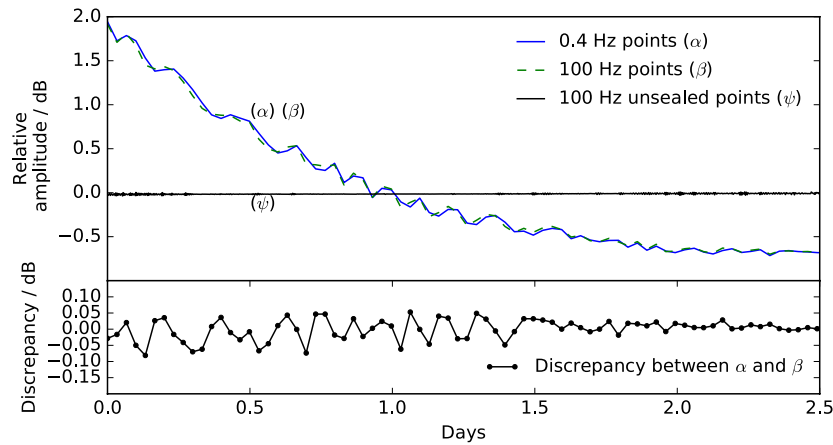
Figure 8. Upper graph: amplitude of electrical transfer function as function of time (days) relative to respective average values (unit: dB) at 0.4 Hz (α) and 100 Hz (β) for properly sealed reciprocity system, and at 100 Hz (ψ) for unsealed reciprocity system. Lower graph: discrepancy (unit: dB) between previously defined relative amplitudes for α and β cases as functions of time (days).

Figure 9. Schematic process for calculation of corrected amplitudes of electrical transfer functions.

cavity was greatly reduced when the reciprocity system was properly sealed. This protocol was essential for eliminating the many cases in which the system was improperly sealed during repeatability measurements.

3.3. Measurement processing

As the cavities and microphones are necessarily sealed, the local environmental variations inside the reciprocity system (i.e. those of the back cavities of the microphones and coupler) have an important effect on its stability. This is true even if the environment inside the static pressure chamber is controlled.

The upper graph in figure 8 is an example of the relative electrical transfer function (relative to the average amplitude) of the sealed reciprocity system at 100 Hz and 0.4 Hz, for measurements repeated sequentially for 2.5 d. The overall amplitude deviation for the sealed reciprocity system was approximately 2.5 dB. In contrast, the same system without sealing (i.e. without the gaskets) produced amplitude deviations lower than ±0.05 dB during the same time period at 100 Hz.

To overcome this problem, a specific measurement process was implemented, based on the hypothesis that the environmental coefficient of the microphone sensitivity (temperature and static pressure) tends towards a fixed value at low frequencies. The lower graph in figure 8 presents the deviation between the amplitude of the electrical transfer function measured at 100 Hz and 0.4 Hz for 2.5 d for the sealed reciprocity system. This graph seems to confirm this hypothesis

by showing an amplitude deviation within ±0.1 dB. Note that this hypothesis is also supported by the literature [29, 30].

Consequently, the process described in figure 9 was implemented to correct the amplitude measurements of the electrical transfer functions. A reference measurement (amplitude C_0) was first conducted for an unsealed reciprocity system (microphones and cavity) at 100 Hz frequency, for which the reciprocity system was not affected by leakage. For the sealed reciprocity system, a measurement at 100 Hz was inserted (amplitudes: B_j, B_{j+1} ...) between two sequential measurements at frequencies of interest. Then, the raw amplitude A_i at frequency f_i was corrected by averaging the adjacent amplitude measurements B_j and B_{j+1} at 100 Hz as an environmental coefficient, and finally, by the reference measurement C_0. Therefore, the amplitudes of the electrical transfer functions measured for the sealed reciprocity system were relative to those measured for the unsealed reciprocity system at 100 Hz, for which the absolute amplitude can be considered reliable. Note that a similar process is not required for phase measurements provided they are unaffected by local environment variations inside the reciprocity system.

To acquire information on the uncertainties, the experiment was designed with multiple sealed cycles and repeatability tests. In accordance with ISO 21748 [31], the following process was implemented as a repeatability test for this experiment:

1 The reciprocity system was installed in the static pressure chamber. It was sealed with five gaskets: one for each microphone (behind the back cavity ring), and three for
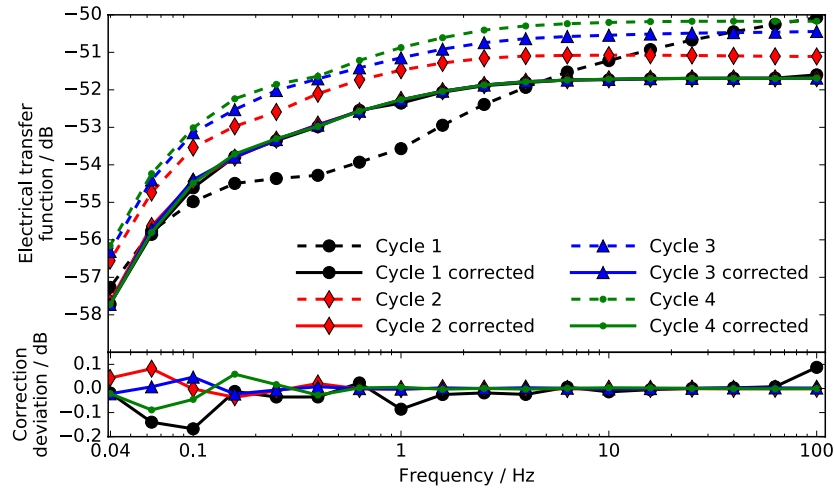
Figure 10. Upper graph: amplitudes (unit: dB) of four raw (dashed lines) and corrected (full lines) electrical transfer functions as functions of frequency. Lower graph: deviation of previously presented corrected electrical transfer functions (unit: dB) relative to the average of the functions without the first cycle, as function of frequency.

the sapphire cylindrical cavity (one at each end of the cavity and one in the static pressure equalisation vent).

2 The system was powered on.

3 The static pressure chamber was closed and regulated at a set-point of 1013 hPa.

4 Thermal balance was expected after 1 h of rest.

5 Cycle measurements were performed without opening the entire system. Each cycle corresponded to sequential generation of sinusoidal signals from 100 Hz to 0.04 Hz, alternating reference points at 100 Hz. A cycle was designed to last 1 h.

6 A minimum of four cycles were implemented for each repeatability test.

7 After the last cycle finished, the system was switched off and unplugged and all gaskets were removed.

8 The cavity was changed and the repeatability test was restarted. A minimum of six repeatability tests were performed for each cavity.

Figure 10 presents raw measurements of the electrical transfer impedance in the frequency range of 100 Hz to 0.04 Hz for four cycles of one repeatability test. The corrected amplitudes are also shown. Although the first cycle of each repeatability test was well corrected (as indicated for the sample repeatability test by the black lines with filled dots in figure 10), they were not retained in the processing. The processing consisted of calculating the defined error estimator δ_m (34) by averaging the corrected electrical transfer functions of the cycles and repeatability tests. A minimum of six repeatability tests were performed for each cavity. This measurement method allowed uncertainty measurements of approximately 0.25 dB at 0.04 Hz. Overall, the measurement period was 12 d.

4. Results and discussion

Figure 11 shows the error estimator δ_m as defined in (34) as a function of frequency, for the acoustic transfer admittances

derived from the formulations discussed in 2.4. The uncertainties are mainly due to the repeatability process.

Analysis of the error estimator δ_m results yields the following findings:

(a) If δ_m does not tend towards zero (unit: dB), the estimated $M_t M_r$ depends on the cavity dimensions. Thus, the formulation of the acoustic transfer admittance is invalid.

(b) If δ_m tends towards zero (unit: dB), the estimated $M_t M_r$ does not depend on the cavity dimensions. Thus, the formulation of the acoustic transfer admittance is valid.

(c) Other unknown and unaccounted for effects somehow compensate for each other by coincidence, for the chosen coupler sizes. However, such possibility appears to be unlikely.

It is worth noting that, for case (b), the formulation can be considered as valid provided the cavity lengths are sufficiently different that the effects under investigation (here, the heat conduction effects) can be measured. This hypothesis was verified in the present study (see section 3.2).

It is clearly apparent from figure 11 that, among the studied formulations, the *general alternative low-frequency solution* (30) is the unique valid model in the targeted frequency range (for amplitude and phase). It is also reminded here that the results for the phase were obtained without applying the environmental correction process described in the previous section. These results are comparable to those obtained for the amplitude where the correction process has been applied. The polytropic condition that occurs in the frequency range of 0.1–10 Hz (for these cavity dimensions) was well corrected by this formulation. The result provided by the *general alternative low-frequency solution* was calculated using $(m, n) = (100, 100)$ for E_P in (24); convergence study shows results within 0.01 dB for $(m, n) = (17, 17)$ at 100 Hz and $(m, n) = (2, 2)$ at 0.04 Hz. As expected, the *short-term alternative low-frequency solution* (25) provided a better result than the standardised 'low-frequency solution' and 'broadband solution'. These results highlight the limitations of the
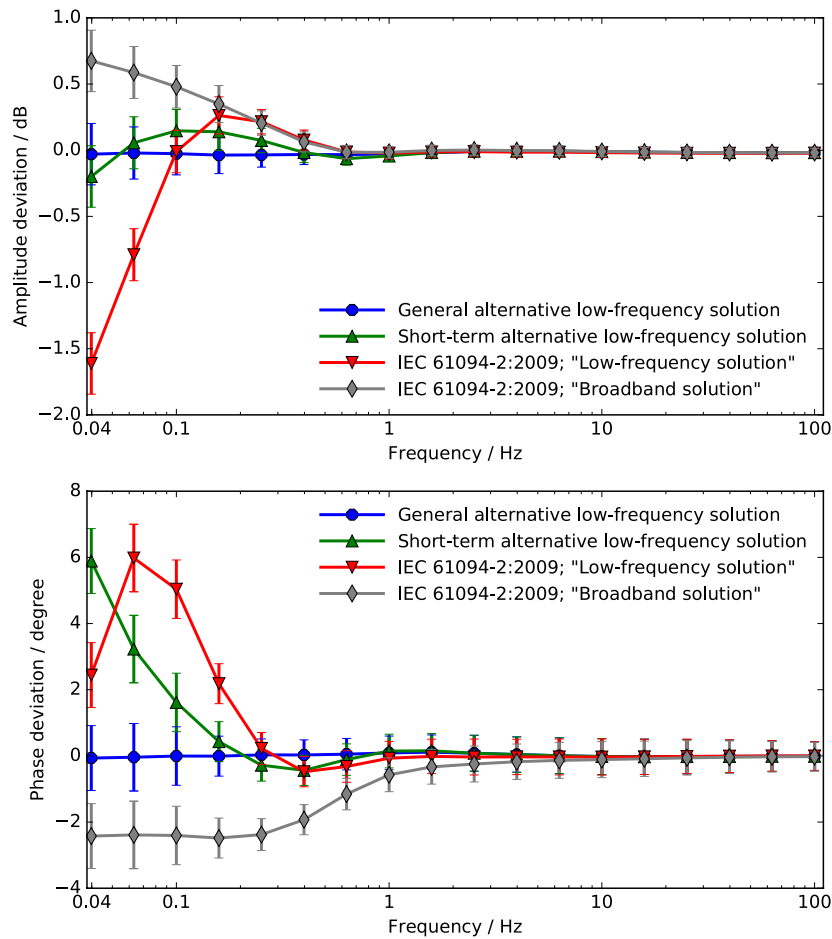
Figure 11. Amplitude (unit: dB, upper graph) and phase (unit: degrees, lower graph) of error estimator δ_m as function of frequency for four different acoustic transfer admittance formulations.
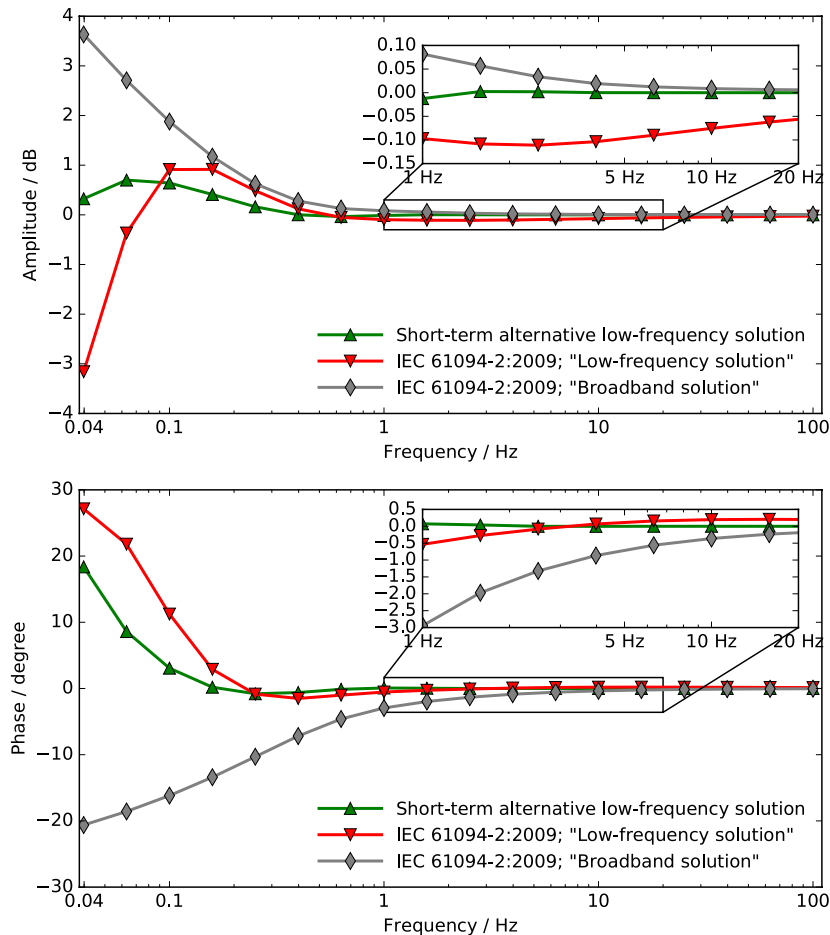
current standardised formulations of acoustic transfer admittance for the purpose of microphone infrasound calibration.

To obtain information on the possible error of microphone calibration using the pressure reciprocity technique, figure 12 presents the acoustic transfer admittances relative to the *general alternative low-frequency solution*, taken here as a reference. As an example, for the standardised 'low-frequency solution', the possible errors in the acoustic transfer admittance, and thus, in $M_t M_r$ reached 0.1 dB and 0.5 degrees at 1 Hz, and up to 3 dB and 30 degrees at 0.04 Hz. The error in the sensitivity estimation was potentially half these values. Therefore, traceability to the International System of Units (SI) for current calibrations is possibly incorrect.

5. Conclusion

The main motivation of this study was to perform groundwork for future primary calibration of microphones in the infrasonic frequency range. Therefore, it was essential to verify the validity of the acoustic transfer admittance formulations for cylindrical cavities at infrasonic frequencies, which are currently standardised and used for primary reciprocity calibration of microphones.

The limitations in the infrasound context of these standardised formulations, i.e. the 'broadband solution' and the 'low-frequency solution', were discussed. In particular, special attention was paid to the 'low-frequency solution', which is based on the 'infinite impedance driver' solution provided by Gerber [13] and which is expected to be valid at low frequencies. Hence, it was found that the presentation of the heat conduction equation as a diffusion equation and the assumption of uniform density variation in the cavity render this approach inappropriate for application to real acoustic situations. Thus, two alternative formulations were proposed in this paper: the *general alternative low-frequency solution* and the *short-term alternative low-frequency solution*. These solutions were both deduced from the 'zero impedance driver' solution for the heat conduction equation provided by Gerber [13]. An experiment performed to test the validity of the formulations discussed in this paper clearly indicated that the *general alternative low-frequency solution* (30) is the only valid model among the studied formulations in the targeted frequency range (for amplitude and phase). From the experiment results, it was also concluded that the *short-term alternative low-frequency solution* (25) yields lower errors than the standardised

Figure 12. Amplitude (unit: dB, upper graph) and phase (unit: degree, lower graph) as functions of frequency for acoustic transfer admittances provided by different formulations (see legend), relative to that provided by *general alternative low-frequency solution* calculated for short cavity coupled with two LS1p microphones.

solutions. Finally, the experiment highlighted the limitations of the current standardised formulations of acoustic transfer admittance for infrasound calibration of microphones.

In conclusion, the models quoted in IEC Standard 61094-2:2009 are not suitable at low frequencies. The following recommendations can be made for future revision of the IEC standard:

(a) The current standardised 'low-frequency solution' should be modified by the *short-term alternative low-frequency solution* as defined in (30) and (25), as the validity of the former solution is limited at low frequencies by the asymptotic development of the general formulation of E_P, presented in (24).

(b) At lower frequencies, where the previous solution is no longer valid, the *general alternative low-frequency solution* should be implemented, as defined in (30) and (24).

The findings of this work have implications for calibration of infrasound sensors, which is particularly important for earth monitoring applications. It would be advisable that in the near future, calibrations of sensors at infrasonic frequencies through reciprocity method as well as other methods

based on closed couplers, such as the laser pistonphone, take into consideration these recommendations.

Appendix A. Environment control

A.1. Static pressure variation control

To protect the sealed microphones against static pressure variations (given the long-term measurements at infrasonic frequencies), a static pressure chamber was designed and manufactured (figure 5). This pressure chamber had a 1 m^3 volume and could be stabilised from 600 hPa to 1100 hPa. During the measurements, the static pressure inside the chamber was regulated at 1013 hPa with variations within ± 0.20 hPa. The static pressure inside the laboratory fluctuated by ± 20 hPa in the vicinity of 1005 hPa.

Figure A1 shows sample results for the static pressure variation inside and outside the regulated chamber for a 10 d period. The static pressure acquisition was performed using a Vaisala PTU301 barometer for the measurements outside the chamber, and with an FHAD 46-C41 digital sensor on an Ahlborn Almemo 2690 station inside the chamber.
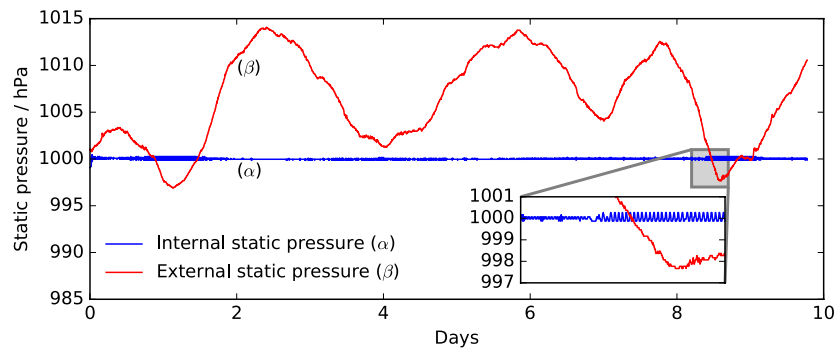
Figure A1. Sample internal (α) and external (β) static pressure variations for regulated chamber as functions of time (days). The static pressure set-point was fixed at 1000 hPa at the beginning of the measurement.
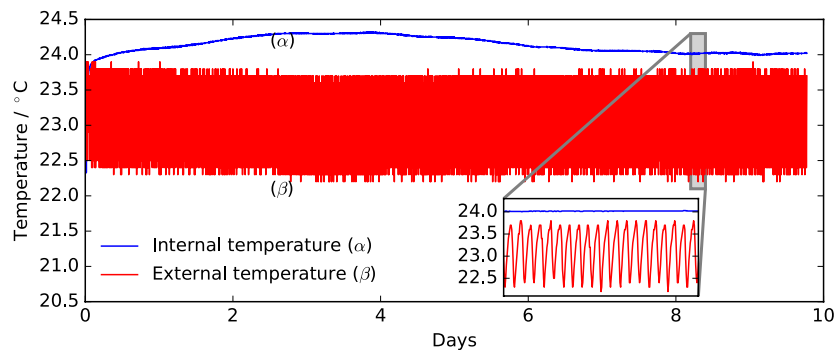
Figure A2. Sample temperature variations inside regulated chamber (α) and in laboratory (β) as functions of time (days). The laboratory temperature set-point was fixed at 23 °C at the beginning of the measurement.

A.2. Temperature variation control

The laboratory temperature was regulated by the air conditioning system with a 15 min regulation period. The static pressure chamber was located in a restricted area closed by a double glass wall that filtered (by a factor of 10) the thermal regulation of the laboratory. Figure A2 shows an example of the internal and external (in the laboratory) temperature conditions of the static pressure chamber for a 10 d period.

The high-frequency temperature amplitude variations were approximately ±0.7 °C in the laboratory and were limited to approximately ±0.3 °C in the static pressure chamber. The temperature acquisition was performed using a Vaisala PTU301 transmitter for the measurements outside the chamber, and with a PT100 sensor on an Ahlborn Almemo 2690 station inside the chamber.

Appendix B. Setup

B.1. Cavities and microphones

Two cavities were designed and manufactured for the experiment: a short (6 mm long) and a long (10 mm long) cavity. Their diameters fit the microphone membranes (18.6 mm, figure 5). The critical dimensions of the cavities were measured at the Laboratoire National de Métrologie et d'Essais (LNE) with uncertainties of ±2 µm. Three gaskets were employed to prevent leakage through the cavitiy: two were placed in a joint groove between the contact planes of the coupler and the front annulus of the microphones, which guaranty the length of the

cavity; the third was placed on the static pressure equalisation vent of the coupler. This vent was especially designed to limit excessive pressure production when closing the volume. A flat gasket was place on each microphone under the serial number back ring in order to seal their static pressure equalisation vent. The installation of this gasket prevents the occurrence of overpressure in the back cavity of the microphone. Figure B1 provides details on how the gaskets are installed in the system.

B.2. Preamplifiers

The receiver microphone was connected to a B&K 2669-L-004 preamplifier with a parallel 100 pF B&K UC0211 capacitance module. This couple was chosen for its low cut-off frequency and good stability. Its technical specifications allowed a sufficiently high signal-to-noise ratio, and allowed repeatability measurements in the infrasonic frequency range because of its short transient response (almost 2 min). The transmitter microphone was connected to a specific preamplifier (infrasound microphone preamplifier (IMP)) designed and manufactured for the experiment (figure 5). Its cut-off frequency was approximately 0.005 Hz because a 500 GΩ polarisation resistor was employed, with added 100 pF capacitance in parallel with the microphone. This design allowed injection of up to 10 V to the transmitter microphone. Because of its very long transient response (almost 1 h), the IMP preamplifier was only used with the transmitter microphone (not the receiver microphone), the electronic behaviour of which provided a shorter transient response in transmitter mode.
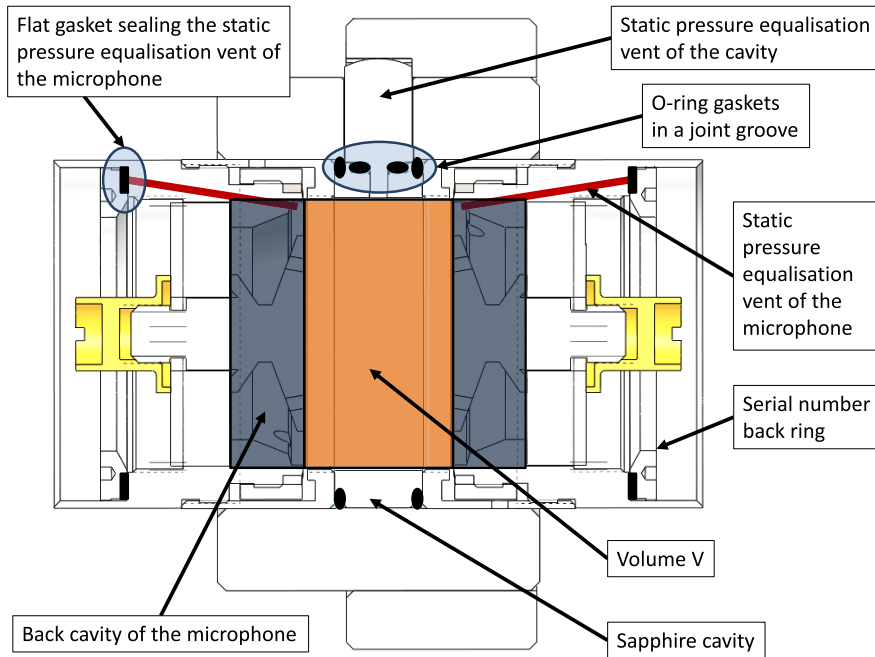
Figure B1. Cross-sectional view of the sapphire cavity and two microphones. Informations are given to show the sealing joints.

Appendix C. Amplitude and phase computation

The amplitude and phase were computed by projection of a digitised signal on the sinusoidal basis, as explained below, inspired by IEEE Standard 1057:2017 [28]. For a digitised sinusoidal signal **y** and assuming that the record contains the sequence of sample $\mathbf{y} = (y_1, ..., y_n)^T$ taken at time instant $t_1, ..., t_n$, it can be further assumed that the data can be modelled as

$$y_n[\chi] = A_0 \cos(\omega t_n) + B_0 \sin(\omega t_n) + C_0, \qquad (C.1)$$

where $\chi = [A_0, B_0, C_0]^T$ is a set of three unknown parameters and ω is the known pulsation. The sine fitting algorithm is implemented by minimising the sum of the squared errors

$$\Gamma[\chi] = \frac{1}{N} \sum_{n=1}^{N} (y_n - y_n[\chi])^2, \qquad (C.2)$$

where y_n is the observation and $y_n[\chi]$ is the modelled sine wave.

By employing vector notation

$$\mathbf{D}(\omega) = \begin{bmatrix} \cos(\omega t_1) & \sin(\omega t_1) & 1 \\ \vdots & \vdots & \vdots \\ \cos(\omega t_N) & \sin(\omega t_N) & 1 \end{bmatrix}, \qquad (C.3)$$

the sum of the squared errors (C.2) can be written as

$$\Gamma(\omega, \chi) = \frac{1}{N} \left(\mathbf{y} - \mathbf{D}(\omega)\chi \right)^T \left(\mathbf{y} - \mathbf{D}(\omega)\chi \right). \quad (C.4)$$

As ω is known, (C.4) is minimised in the least-squares sense by solving the linear equations $\mathbf{D}(\omega)\chi = \mathbf{y}$, which gives the solution

$$\chi_0 = \left(\mathbf{D}(\omega)^T \mathbf{D}(\omega) \right)^{-1} \mathbf{D}(\omega)^T \mathbf{y}. \qquad (C.5)$$

To obtain the amplitude and phase form

$$y_n = A \cos(\omega t_n + \Phi) + C_0, \qquad (C.6)$$

the expressions for the amplitude A and phase Φ of the digitised signal given by the IEEE [28] are used:

$$A = \sqrt{A_0^2 + B_0^2},$$
$$\Phi = -\arctan(B_0, A_0). \qquad (C.7)$$

References

[1] IEC 61094-2:2009 2009 Measurement microphones-Part 2: primary method for the pressure calibration of laboratory standard microphones by the reciprocity method (IEC Standard)
[2] Avison J and Barham R 2014 Final report on key comparison CCAUV.A-K5: pressure calibration of laboratory standard microphones in the frequency range 2 Hz–10 kHz *Metrologia* **51** 09007
[3] BIPM 2018 Acoustics, Ultrasound, Vibration—Calibration and measurement capabilities (Accessed: 8 June 2018) https://kcdb.bipm.org/appendixC/
[4] Molinar G F, Rebaglia B, Sacconi A, Legras J C, Vailleau G P, Schmidt J W, Stoup J R, Flack D R, Sabuga W and Jusko O 1999 Ccm key comparison in the pressure range 0.05 MPa–1 MPa (gas medium, gauge mode). Phase A1: dimensional measurements and calculation of effective area *Metrologia* **36** 657
[5] Stefe M, Svete A and Kutin J 2018 Development of a dynamic pressure generator based on a loudspeaker with improved frequency characteristics *Measurement* **122** 212–9
[6] Zhang F, He W, He L and Rong Z 2015 Acoustic properties of pistonphones at low frequencies in the presence of pressure leakage and heat conduction *J. Sound Vib.* **358** 324–33
[7] NF XP S 31-135 2017 Acoustique—Basses fréquences—Méthode de mesurage. Standard, NF XP S 31-135

[8] DIN 45680:1997-03 1997 Messung und Bewertung tieffrequenter Gerausschimmissionen in der Nachbarschaft. Standard, DIN 45680:1997-03

[9] CTBTO preparatory commission 2004 Operation manual for infrasound monitoring and the international exchange of infrasound data *CTBTO Report* CTBTO

[10] BIPM 2017 Strategy 2017–2027, Consultative committee for acoustics, ultrasound, and vibration (CCAUV) *Technical report* BIPM

[11] Daniels F 1947 Acoustical impedance of enclosures *J. Acoust. Soc. Am.* **19** 569–71

[12] Biagi F and Cook R 1954 Acoustic impedance of a right circular cylindrical enclosure *J. Acoust. Soc. Am.* **26** 506–9

[13] Gerber H 1964 Acoustic properties of fluid-filled chambers at infrasonic frequencies in the absence of convection *J. Acoust. Soc. Am.* **36** 1427–34

[14] Riéty P and Lecollinet M 1974 Le dispositif d'étalonnage primaire des microphones de laboratoire de l'institut national de métrologie *Metrologia* **10** 17

[15] Ballagh K O 1987 Acoustical admittance of cylindrical cavities *J. Sound Vib.* **112** 567–9

[16] Jarvis D R 1987 Acoustical admittance of cylindrical cavities *J. Sound Vib.* **117** 390–2

[17] Rasmussen K 2004 Datafiles sismulating a pressure reciprocity calibration of microphones *EUROMET Project 294—Report* PL-13a

[18] Guianvarc'h C, Durocher J-N, Bruneau M and Bruneau A-M 2006 Acoustic tranfer admittance of cylindrical cavities *J. Sound Vib.* **292** 595–603

[19] Olsen E and Frederiksen E 2013 Microphone acoustic impedance in reciprocity calibration of laboratory standard microphone *INTER-NOISE and NOISE-CON Congress and Conf. Proc.* vol 247 pp 679–86

[20] Jackett R 2014 The effect of heat conduction on the realization of the primary standard for sound pressure *Metrologia* **51** 423

[21] Svete A, Bajsic I and Kutin J 2018 Investigation of polytropic corrections for the piston-in-cylinder primary standard used in dynamic calibrations of pressure sensors *Sensors Actuators* A **274** 262–71

[22] IEC 327:1971 1971 *Precision Method for Pressure Calibration of One-inch Standard Condenser Microphones by the Reciprocity Technique.* (IEC Standard)

[23] Zwikker C and Kosten C 1949 *Sound Absorbing Materials* (Amsterdam: Elsevier)

[24] IEC 61094-2:1992 1992 *Measurement Microphones-Part 2: Primary Method for the Pressure Calibration of Laboratory Standard Microphones by the Reciprocity Method.* (International Organization for Standardization)

[25] Guianvarc'h C 2005 La cavité de couplage acoustique dans la méthode de réciprocité: modèles analytiques pour l'étalonnage des microphones et la mesure d'impédances de petits composants *PhD Thesis* Le Mans

[26] Bruneau M, Herzog P, Kergomard J and Polack J D 1989 General formulation of the dispersion equation in bounded visco-thermal fluid, and application to some simple geometries *Wave Motion* **11** 441–51

[27] Rasmussen K 1993 Radial motion-wave in cylindrical plane-wave couplers *Acta Acust.* **1** 145–51

[28] IEEE 1057:2017 2017 *Standard for Digitizing Waveform Recorders* (IEEE Standard)

[29] Rasmussen K 2001 Properties and calibration of laboratory standard microphones *Technical report* B&K

[30] Rasmussen K 1999 The static pressure and temperature coefficients of laboratory standard microphones *Metrologia* **36** 265

[31] ISO 21748:2017 2017 *Guidance for the Use of Repeatability, Reproducibility and Trueness Estimates in Measurement Uncertainty Evaluation* (International Organization for Standardization)